Available online at www.sciencedirect.com

ScienceDirect

Physics Procedia 57 (2014) 58 – 67

Physics Procedia

Negative-weight percolation: review of existing literature and scaling behavior of the path weight in 2*d*

O. Melchert, C. Norrenbrock, A. K. Hartmann

Institut für Physik, Universität Oldenburg, Carl-von-Ossietzky Strasse, 26111 Oldenburg, Germany

Abstract

We consider the negative weight percolation (NWP) problem on hypercubic lattice graphs with fully periodic boundary conditions in all relevant dimensions from $d = 2$ to the upper critical dimension $d = 6$. The problem exhibits edge weights drawn from disorder distributions that allow for weights of either sign. We are interested in the statistical properties of the full ensemble of loops with negative weight, i.e. non-trivial (system spanning) loops as well as topologically trivial ("small") loops that comprise the "loops only" variant of the NWP problem. The NWP phenomenon refers to the disorder driven proliferation of system spanning loops of total negative weight. For the numerical simulations we employ a mapping of the NWP model to a combinatorial optimization problem that can be solved exactly by using sophisticated matching algorithms. This allows for the numerically exact study of large systems with good statistics, important to ensure a reliable disorder average.

Early simulations for the 2*d* setup led to suggest that the resulting negative-weight percolation (NWP) problem is fundamentally different from conventional percolation. Here, we review several studies that reported on results of numerical simulations aimed at clarifying the geometric properties of NWP on hypercubic lattice graphs and random graphs.

Finally we present additional new results for the scaling behavior of the geometric properties and the configurational weight of minimum-weight paths (MWPs) in the "loops + MWP" variant of the model, characterizing an additional threshold ρ_c^{ω}, above which the disorder averaged MWP weight $\langle \omega_p \rangle$ is negative, thereby highlighting a characteristic limiting case of the NWP model at small densities of negative edges.

Peer-review under responsibility of The Organizing Committee of CSP 2014 conference
Keywords: minimum-weight paths, percolation, phase transitions, finite-size scaling analysis
PACS: 64.60.ah, 64.60.De, 05.10-a

1. Introduction

The statistical properties of lattice-path models on graphs, equipped with quenched disorder, have experienced much attention during the last decades. They have proven to be valuable in order to describe line-like quantities as, e.g., linear polymers in disordered/random media (Kremer, 1981; Kardar and Zhang, 1987; Derrida, 1990; Grassberger, 1993; Parshani et al., 2009), vortex loops in high-T_c superconductivity at zero field (Nguyen and Sudbø, 1998, 1999; Pfeiffer and Rieger, 2002, 2003) and the $d = 3$ XY model (Kajantie et al., 2000; Camarda et al., 2006), networks

E-mail addresses: oliver.melchert@uni-oldenburg.de (O. Melchert)., christoph.norrenbrock@uni-oldenburg.de (C. Norrenbrock)., alexander.hartmann@uni-oldenburg.de (A. K. Hartmann).

Peer-review under responsibility of The Organizing Committee of CSP 2014 conference
doi:10.1016/j.phpro.2014.08.132

of vortex strings found after a symmetry-breaking phase transition in field theories (Antunes and Bettencourt, 1998; Hindmarsch and Strobl, 1995; Strobl and Hindmarsh, 1997), as well as domain wall excitations in disordered media such as spin glasses (Cieplak et al., 1994; Melchert and Hartmann, 2007) and the solid-on-solid model (Schwarz et al., 2009). The actual computation of the underlying paths can often be formulated in terms of a combinatorial optimization problem and hence might allow for the application of exact optimization algorithms developed in computer science (Schwartz et al., 1998; Papadimitriou and Steiglitz, 1998; Rieger, 2003; Hartmann, 2007). So as to analyze the statistical properties of these lattice path models, geometric observables and scaling concepts similar to those used in percolation theory (Stauffer, 1979; Stauffer and Aharony, 1994) and other "string"-bearing models (Allega et al., 1990; Austin et al., 1994; Schakel, 2001) are often applicable. To give a brief account of the former: the pivotal issue of standard percolation is that of connectivity. A basic example is $2d$ random bond percolation, where one studies a lattice in which a random fraction of the edges is "occupied". Clusters composed of adjacent sites joined by occupied edges are then analyzed regarding their geometric properties. Depending on the precise fraction of occupied edges, the geometric properties of the clusters change, leading from a phase with rather small and disconnected clusters to a phase, where there is basically one large cluster covering the lattice. Therein, the appearance of an infinite, i.e. percolating, cluster is described by a second-order phase transition.

The focus of the presented article is the *negative-weight percolation* (NWP) model (Melchert and Hartmann, 2008; Apolo et al., 2009; Melchert et al., 2010; Melchert and Hartmann, 2013; Claussen et al., 2012; Norrenbrock et al., 2013; Mitran et al., 2013), a problem with subtle differences as compared to other string-like percolation problems. So as to study one of the most basic setups of the corresponding NWP problem, one might consider a regular lattice graph with periodic boundary conditions (BCs) where adjacent sites are joined by undirected edges. Weights are assigned to the edges, representing quenched random variables drawn from a distribution that allows for edge weights of either sign. The details of the weight distribution are further controlled by a tunable disorder parameter ρ (for a more detailed discussion, see Subsect. 2.1). For a given realization of the disorder, one then computes a configuration of loops, i.e. closed paths on the lattice graph, such that the total sum of the weights assigned to the edges that build up the loops attains an *exact* minimum. Thus, no loops with positive weight will appear. In addition, one might force an additional path on the lattice, for which one might further fix its terminal points. Note that the application of exact algorithms in contrast to standard sampling approaches like Monte Carlo simulations avoids, e.g., equilibration problems. Also, since the algorithms run in polynomial time, large instances can be solved. As an additional optimization constraint we impose the condition that the loops are not allowed to intersect; consequently there is no definition of clusters in the NWP model. Regardless of the spatial dimension of the underlying graph, the observables are always line-like, i.e. have an intrinsic dimension of $d = 1$. Nevertheless, the loops may be fractal with fractal dimensions $d_f > 1$. Since a loop does neither intersect with itself nor with other loops in its neighborhood, it exhibits an "excluded volume" quite similar to usual self avoiding walks (SAWs) (Stauffer and Aharony, 1994). The problem of finding these loops can be cast into a minimum-weight path (MWP) problem, outlined below in Subsect. 2.1 in more detail.

As a pivotal observation it was found that, as a function of the disorder parameter ρ, the NWP model features a disorder driven, geometric phase transition, triggered by a sudden change of the typical loop size (Melchert and Hartmann, 2008) (as discussed below in more detail). In this regard, depending on the precise lattice setup and on the value of ρ, one can identify two different phases: (i) a phase where the loops are "small", meaning that the linear extensions of the loops are small in comparison to the system size, see Fig. 1(a) (therein, the linear extension of a loop refers to its projection onto the independent lattice axes), resembling a dilute gas of loops, and, (ii) a phase where "large" loops exist that comprise densely packed configurations of loops and eventually span the entire lattice, see Fig. 1(c). Regarding these two phases and in the limit of large system sizes, there is a particular value of the disorder parameter, signified as ρ_c, at which system spanning (or "percolating") loops appear for the first time, see Fig. 1(b).

Previously, we have investigated the NWP phenomenon for hypercubic lattice graphs in dimensions 2 through 6 (Melchert and Hartmann, 2008; Melchert et al., 2010) using finite-size scaling (FSS) analyses, where we characterized the underlying transition by means of a whole set of critical exponents. The respective studies are summarized below in Sect. 2. Considering different disorder distributions and lattice geometries, the exponents were found to be universal in $2d$ and clearly distinct from those describing standard percolation phenomena. Further, the studies on hypercubic lattice graphs suggested that the upper critical dimension of the NWP model is $d_u = 6$ (see Subsect. 2.2). This finding was later supported by considering the model on regular random graphs, giving direct access to the mean-field behavior of the NWP problem, and by an analytic approach that utilizes a correspondence between the NWP problem

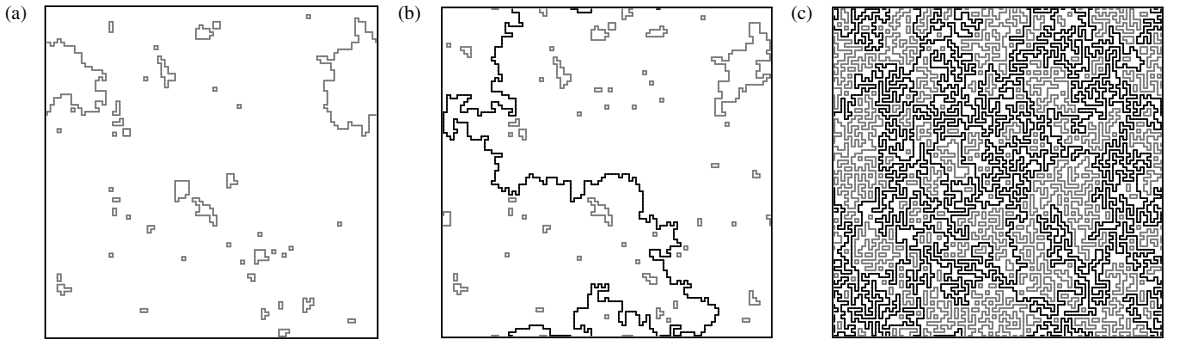

Fig. 1. Samples of loop configurations for a $2d$ square lattice with side length $L = 96$ and periodic boundary conditions, illustrating the NWP phenomenon. Percolating (nonpercolating) loops are colored black (gray). The snapshots relate to different values of the disorder parameter ρ, where (a) $\rho < \rho_c$, (b) $\rho \approx \rho_c$, and, (c) $\rho > \rho_c$. In the limit of large system sizes and above the critical point ρ_c, paths might span the lattice along any direction with the periodic boundaries.

and the problem of polymers in random media, see Subsect. 2.3. For the particular case of the $2d$ NWP problem we studied the effect of dilution on the critical properties of the $2d$ NWP phenomenon, see Subsect. 2.4, and checked whether NWP lattice paths can be described by SLE (see Subsect. 2.5). We further studied densely and fully packed configurations of loops as limiting cases of the NWP problem at extremal disorder, see Ref. (Melchert and Hartmann, 2011b), utilized the NWP algorithm to devise an algorithm that yields groundstate spin configurations for the planar $2d$ triangular random bond Ising model (Melchert and Hartmann, 2011a), and used a Migdal-Kadanoff approximation scheme to study the NWP problem on disordered hierarchical graphs with effective dimension $d = 2.32$ (Melchert and Hartmann, 2013). Recently, we analyzed a variety of local optimization approaches to study the $2d$ NWP problem by using a dynamical random-walk approach (Mitran et al., 2013). However, due to space limitations, these latter studies are not reviewed here further.

The remainder of the presented article is organized as follows. In Sect. 2, we introduce the model in more detail and review some of the existing literature on the NWP problem. In Sect. 3, we present new results related to the scaling behavior of the path weight in the $2d$ NWP problem. Finally, Sect. 4 concludes with a brief summary.

2. NWP on hypercubic lattices

In the subsequent section, we first consider the intuitive case of a $2d$ square lattice in order to introduce the precise NWP problem statement and to describe the algorithm we devised to yield minimum-weight configurations of loops and paths. In Subsects. 2.2 through 2.5, we then briefly recap some studies on the NWP problem.

2.1. The NWP Problem: Problem setup and algorithm

Below we consider lattice graphs $G = (V, E)$, where V and E signify the node-set and edge-set of a graph, respectively. Except for Subsect. 2.3, where we consider r-regular random graphs, we consider hypercubic lattice graphs of side length L and fully periodic boundary conditions (BCs) in dimensions $d = 2$ through 6. These graphs have $N = |V|$ sites (in case of hypercubic lattices one has $N = L^d$) $i \in V$ and a number of $m = |E|$ undirected edges $\{i, j\} \in E$ that join adjacent sites $i, j \in V$. We further assign a weight ω_{ij} to each $\{i, j\} \in E$. These weights represent independent identically distributed (IID) quenched random variables that introduce disorder to the lattice. Here, we consider IID weights which either have a unit weight (probability 1-ρ) or are drawn (probability ρ) from a Gaussian distribution with zero mean and variance one. The respective disorder distribution reads

$$P(\omega) = \rho \exp\left(-\omega^2/2\right)/\sqrt{2\pi} + (1-\rho)\delta(\omega - 1), \tag{1}$$

and it explicitly allows for loops $\mathcal{L} \subset E$ with a negative total weight $\omega_{\mathcal{L}} = \sum_{\{i,j\}\in\mathcal{L}} \omega_{ij}$. Note that in previous studies on NWP also strictly bimodal $\pm J$ edge-weight distributions where considered (Melchert and Hartmann, 2008). To

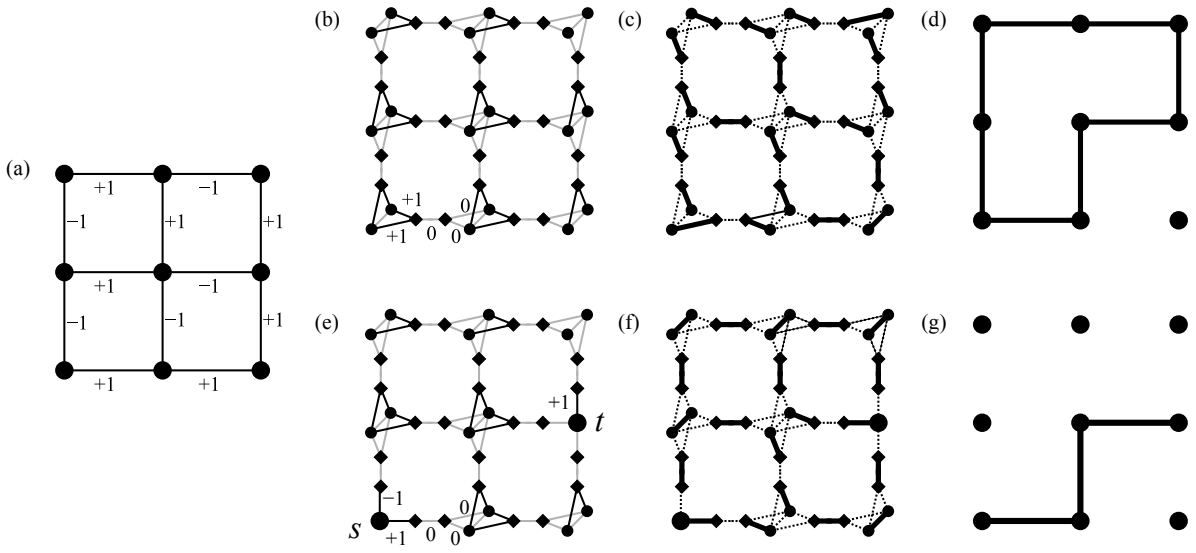

Fig. 2. Illustration of the algorithmic procedure: (a) original lattice G with edge weights, (b) auxiliary graph G_{A} with proper weight assignment. Black edges carry the same weight as the respective edge in the original graph and grey edges carry zero weight, (c) minimum-weight perfect matching (MWPM) M: bold edges are matched and dashed edges are unmatched, and (d) loop configuration (bold edges) that corresponds to the MWPM depicted in (c). Further, the following subfigures illustrate the changes in the algorithmic procedure to obtain a minimum weight s-t-path: (e) auxiliary graph G_{A}, where the mapping is modified to induce a minimum weight path that connects nodes s and t. Black edges carry the same weight as the respective edge in the original graph and grey edges carry zero weight, (g) corresponding MWPM, (f) minimum weight path (bold edges) that corresponds to a MWPM on G_{A}. For the particular example illustrated here, the path has weight $\omega_p = -1$ and there are no loops in addition to the path.

support intuition: For any nonzero value of the *disorder parameter* ρ, a sufficiently large lattice will exhibit at least "small" loops that exhibit a negative weight, see Fig. 1(a). If the disorder parameter is large enough, system spanning loops with negative weight will exist, see Figs. 1(b-c).

The NWP problem statement then reads as follows: Given G together with a realization of the disorder, determine a set C of loops such that the configurational energy, defined as the sum of all the loop-weights $\mathcal{E} = \sum_{\mathcal{L}\in C} \omega_{\mathcal{L}}$, is minimized. As further optimization constraint, the loops are not allowed to intersect and generally, the weight of an individual loop is smaller than zero. Note that C may also be empty (clearly this is the case for $\rho = 0$). The configurational energy $\mathcal{E}$ is the quantity subject to optimization and the result of the optimization procedure is a set of loops C, obtained using an appropriate transformation of the original graph as detailed in Ref. (Ahuja et al., 1993). So as to identify the edges that constitute the loops for a particular instance of the disorder, we can benefit from a relation between minimum-weight paths (and loops) on G and minimum-weight perfect matchings (MWPM) (Cook and Rohe, 1999b; Hartmann and Rieger, 2001; Melchert, 2009) on the transformed graph. Here, we give a brief description of the algorithmic procedure that yields a minimum-weight set of loops for a given realization of the disorder. Fig. 2 illustrates the 3 basic steps, detailed below:

(1) each edge, joining adjacent sites on the original graph G, is replaced by a path of 3 edges. Therefore, 2 "additional" sites have to be introduced for each edge in E. Therein, one of the two edges connecting an additional site to an original site gets the same weight as the corresponding edge in G. The remaining two edges get zero weight. The original sites $i \in V$ are then "duplicated", i.e. $i \to i_1, i_2$, along with all their incident edges and the corresponding weights. For each of these pairs of duplicated sites, one additional edge $\{i_1, i_2\}$ with zero weight is added that connects the two sites i_1 and i_2. The resulting auxiliary graph $G_{\mathrm{A}} = (V_{\mathrm{A}}, E_{\mathrm{A}})$ is shown in Fig. 2(b), where additional sites appear as squares and duplicated sites as circles. Fig. 2(b) also illustrates the weight assignment on the transformed graph G_{A}. A more extensive description of the mapping can be found in Refs. (Melchert and Hartmann, 2007; Ahuja et al., 1993).

(2) a MWPM on the auxiliary graph is determined via exact combinatorial-optimization algorithms (Cook and Rohe, 1999a,b). A MWPM is a minimum-weighted subset M of E_{A}, such that each site contained in V_{A} is met by

precisely one edge in M. This is illustrated in Fig. 2(c), where the solid edges represent M for the given weight assignment. The dashed edges are not matched.

(3) finally it is possible to find a relation between the matched edges M on G_{A} and a configuration of negative-weighted loops C on G by tracing back the steps of the transformation (1). As regards this, note that each edge contained in M that connects an additional site (square) to a duplicated site (circle) corresponds to an edge on G that is part of a loop, see Fig. 2(d). More precisely, there are always two such edges in M that correspond to one loop segment on G. All the edges in M that connect like sites (i.e. duplicated-duplicated, or additional-additional) carry zero weight and do not contribute to a loop on G. Once the set C of loops is found, a depth-first search (Ahuja et al., 1993; Hartmann and Rieger, 2001) can be used to identify the loop set C and to determine the geometric properties of the individual loops. For the weight assignment illustrated in Fig. 2(a), there is only one negative weighted loop with $\omega_{\mathcal{L}} = -2$ and length $\ell = 8$.

Note that the result of the calculation is a collection C of loops such that the total loop weight, and consequently the configurational energy $\mathcal{E}$, is minimized. Hence, one obtains a global collective optimum of the system. Obviously, all loops that contribute to C possess a negative weight. Also note that the above description explains how to obtain a set of loops only. If one aims to compute an additional minimum weight path (MWP) that connects two nodes, say s and t, on the graph, the transformation procedure for these two particular nodes will look slightly different. I.e. the duplication step introduced in step (1) will be skipped for nodes s and t, see Fig. 2(e). Computing a MWPM for the resulting graph will then yield a minimum weight path that connects nodes s and t together with a set of loops (the set might be empty) as explained in steps (2) and (3) above. This is illustrated in Figs. 2(f-g), where for the same weight assignment as in Fig. 2(a), a minimum weight path is computed. The algorithmic procedure extends to the r-regular random graphs, discussed in Subsect. 2.3 below, in a straight-forward manner.

2.2. A recap of results in dimensions 2 through 7

By means of numerical simulations we characterized the NWP phase transition and geometric properties of minimum-weight paths and loops by observables from percolation theory (Stauffer, 1979; Stauffer and Aharony, 1994). While studies on the NWP minimum-weight path setup were done in $2d$ only (Melchert and Hartmann, 2008), the NWP loop setup was considered on hypercubic lattice graphs in dimensions $d = 2$ through 7 (Melchert et al., 2010). For each setup, we determined the critical exponents of the corresponding geometric phase transitions using finite-size scaling analyses for the percolation probability and the order parameter related observables. It turned out that, for any dimension, the obtained exponents differ from those of commonly studied string-percolation models and satisfy the hyper-scaling relations $d_f = d - \beta/\nu$ and $\gamma + 2\beta = d\nu$, which are known from percolation theory. From various setups and disorder distributions considered in $2d$ (Melchert and Hartmann, 2008) and $3d$ (Melchert and Hartmann, 2008; Melchert et al., 2010), we conclude that the critical exponents are universal. That means they do not depend on the subtleties of the disorder, i.e. discrete of continuous, or the particular lattice geometry, i.e. square or hexagonal. Furthermore, we found that the results obtained from the numerical simulations in higher dimensions are consistent with an upper critical dimension $d_u = 6$ (Melchert et al., 2010).

2.3. Mean field behavior of the NWP model

The issue of the upper critical dimension in the NWP model was further addressed by means of a complementary approach in Ref. (Melchert et al., 2011). Therein we considered minimum-weight loops and paths in the NWP problem on $r = 3$-regular random graphs (3RRGs), where each node has exactly 3 neighbors and where there is no regular lattice structure. On such graphs one has direct access to the mean-field exponents that govern the model for $d \geq d_u$. For each of the graph we first determined the diameter R_N, i.e. the longest among all shortest paths (measured in node-to-node hops). Then we obtained the minimum weight path that connects two nodes separated by distance R_N. It can be expected that $\langle \ell \rangle \propto R_N$ for $\rho \to 0$ and $\langle \ell \rangle \propto N$ for $\rho \to 1$, where $\langle \ell \rangle$ denotes the disorder averaged length of the minimum-weight path. In between, there should be a critical value ρ_c, where the string-like observables exhibit the same scaling behavior as completely uncorrelated random walks. Thus, at ρ_{c} the minimum weight path is expected to scale as $\langle \ell \rangle \propto R_N^2$. As reported in Ref. (Melchert et al., 2011), the critical point $\rho_c = 0.075(1)$ has been obtained by a scaling analysis of the probability P_N^{ω} that the path weight ω_{p} is ≤ 0. Furthermore, several critical exponents have been found and the critical point could be confirmed by an analytic approach using the replica symmetric cavity

method and a correspondence between the NWP problem and the problem of polymers in random media. In either case, the results were in agreement with those found for the 6d hypercube.

2.4. Phase transitions in diluted negative weight percolation models

Particularly for the case of the 2d square lattice, we investigated the effect of dilution, i.e. additional disorder that affects the topology of the underlying lattice graphs, on the critical properties of NWP. Therefore, we used observables from percolation theory (Stauffer, 1979; Stauffer and Aharony, 1994) and a finite-size-scaling analysis in order to identify critical lines in the disorder-dilution plane for two different types of dilution. In this regard we distinguish: (i) Type I dilution, where the disorder is characterized by a fraction p_{I} of edge weights $\omega_{ij} = 0$. (ii) Type II dilution: The lattice is diluted by a fraction p_{II} of *absent* bonds. It was found that, in contrast to type I, type II dilution changes the universality class of NWP. A more detailed analysis of the critical exponents for one particular critical point, i.e. $(\rho, p_{\mathrm{II}}) = (1.0, 0.4998)$, verified that the exponents are connected by the usual scaling relations known from scaling theory. Moreover, the value of the fractal dimension d_f found for the negative-weighted loops at that particular critical point agrees well with the fractal dimension of self avoiding walks on a regular lattice ($d_f^{\mathrm{SAW}} = 4/3$), suggesting that negative weighted loops at $(\rho, p_{\mathrm{II}}) = (1.0, 0.4998)$ belong to the same universality class as 2d self-avoiding walks.

2.5. SLE properties of the 2d NWP problem

For the particular case of the "loops + minimum weight path" variant of the 2d NWP problem, Ref. (Norrenbrock et al., 2013) summarizes a study which addresses the question whether minimum-weight paths in the NWP model might be described in terms of Schramm-Loewner evolution (SLE). Several numerical studies which take the geometrical properties of the NWP path into account lead to different estimates of the diffusion constant κ, which, as a single parameter, characterizes SLE curves. Consequently, it can be ruled out that these paths can be described in terms of SLE. As pointed out in (Norrenbrock et al., 2013), this might be due to a validation of the so-called "Markov-property" (Cardy, 2005).

3. The scaling behavior of the path weight in the 2d NWP problem

In the majority of the NWP related studies, reviewed above, the focus was set on the disorder driven phase transition at which system spanning loops emerge. However, in the seminal NWP study (Melchert and Hartmann, 2008) it was found that there appears to be another value of the disorder parameter ρ, which seems to be interesting from a point of view of statistical physics. Considering a loops + minimum-weight path (MWP) setup in 2d with periodic boundary conditions (BCs) in one direction, it was found that prior to the critical point ρ_{c}, a particular transition point $\rho_{\mathrm{c}}^{\omega}$ exists that indicates a value of the disorder parameter above which (in the limit $L \to \infty$) the ensemble averaged path weight $\langle \omega_{\mathrm{p}} \rangle$ turns negative for the first time. While ρ_{c} can be located by monitoring the *geometric* properties of the loops and MWPs, $\rho_{\mathrm{c}}^{\omega}$ can be located by monitoring the *configurational weight* of the MWPs. To support intuition, for $\rho < \rho_{\mathrm{c}}^{\omega}$ there are only few edges with a negative weight and $\langle \omega_{\mathrm{p}} \rangle > 0$, see Fig. 3(a). However, for $\rho > \rho_{\mathrm{c}}^{\omega}$ there are enough negative weighted edges to ensure $\langle \omega_{\mathrm{p}} \rangle < 0$. For $\rho > \rho_{\mathrm{c}}$, the MWPs eventually get long enough to also span the lattice along the direction with the periodic BCs, see Fig. 3(b), and, finally, the configurations get more "dense" as $\rho \to 1$, see Figs. 3(c-d). To recap the results reported in Ref. (Melchert and Hartmann, 2008): considering a bimodal weight distribution, the particular values $\rho_{\mathrm{c}}^{\omega} = 0.0869(2)$ and $\rho_{\mathrm{c}} = 0.1032(5)$ were found. Nevertheless, in Ref. (Melchert and Hartmann, 2008) only a thorough finite-size with regards to the geometric transition was performed.

Thus, to do this for the transition concerning the weights of the paths, here we perform numeric simulations for the loops + MWP setup for a 2d square lattice with periodic BCs in one direction, distinguishing three types of MWPs (the algorithmic procedure that allows to implement MWPs is discussed in Subsect. 2.1):

(i) MWP-1, where both terminal nodes of the MWP are allowed to terminate along the free boundaries, see Fig. 3,
(ii) MWP-2, where the location of one terminal node is fixed at a randomly chosen node along the associated free boundary,
(iii) MWP-3, where both terminal nodes are fixed at a pair of randomly chosen opposing nodes along the free boundaries.

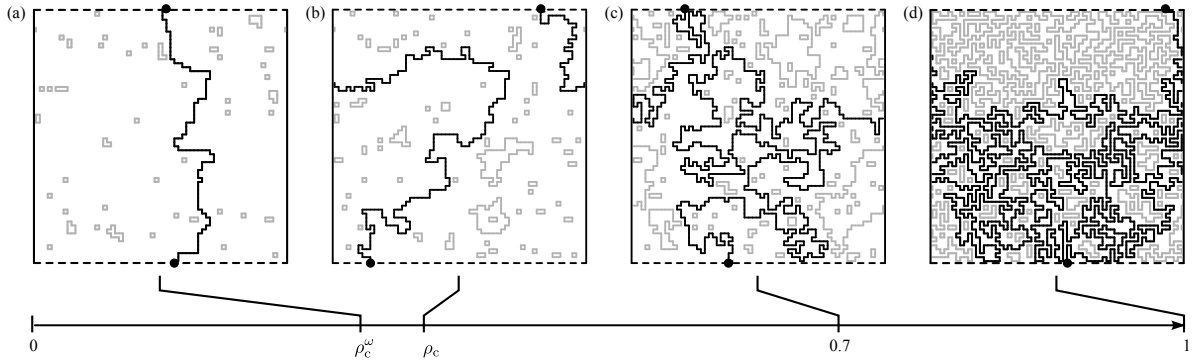

Fig. 3. Samples of "loops+MWP" configurations on $2d$ square lattice with side length $L = 64$, illustrating the NWP phenomenon considering the MWP-1 setup. Solid (dashed) boundary lines indicate periodic (free) boundary conditions. The MWP is colored in black and its terminal nodes are indicated by a black dot, the loops are colored gray. The snapshots relate to different values of the disorder parameter ρ, where (a) $\rho = \rho_c^\omega = 0.285(1)$ (see text for details), (b) $\rho \approx \rho_c = 0.340(1)$, (c) $\rho = 0.7$, and (d) $\rho = 1$. The bottom part illustrates the location of the different configurations along the "disorder scale" from $\rho = 0 \ldots 1$.

We further consider a disorder distribution of the form of Eq. (1), i.e.

$$P(\omega) = \rho \exp(-\omega^2/2)/\sqrt{2\pi} + (1-\rho)\delta(\omega - 1), \tag{2}$$

for which we subsequently estimate the associated value of ρ_c^ω for each of the above three MWP setups, see Subsect. 3.1. Once the values of ρ_c^ω are determined, we perform further simulations to also assess the scaling properties of the MWP configurational weight ω_p (or, to be more precise, the sample-to-sample fluctuation thereof), MWP length ℓ and MWP width (or roughness) r, see Subsect. 3.2.

3.1. Location of the transition point ρ_c^ω

In order to locate the transition points ρ_c^ω, above which the ensemble averaged MWP weight $\langle\omega_p\rangle$ turns negative for the three different MWP setups introduced above, we monitored the average path weight as a function of the disorder value ρ. The location of the NWP critical point for the considered disorder distribution, i.e. $\rho_c = 0.340(1)$, and the fact that $\rho_c^\omega < \rho_c$ can further serve as a guide to set proper ρ-values for the simulations. We considered systems of size $L = 24 \ldots 128$ and up to 12800 realizations of the disorder to compute averages. The decrease of the average MWP weight for increasing values of ρ for all three MWP setups is shown in the main plot of Fig. 4(a). As evident from the data curves that correspond to, say, setup MWP-3, the effective transition points $\rho_{\text{eff}}(L)$ at which the path weight turns negative decrease with increasing system size L. So as to extrapolate to the limit $L \to \infty$, we fit a 4th-order polynomial to the individual data curves to precisely estimate the effective transition points and subsequently assess the asymptotic values ρ_c^ω by assuming a scaling of the form

$$\rho_{\text{eff}}(L) = \rho_c^\omega + aL^{-b} \,. \tag{3}$$

The respective finite-size scaling is shown in the inset of Fig. 4(a). As evident from the figure, the MWP-1 setup, i.e. the setup with the "free ends", exhibits a different scaling exponent b than the other two setups. Using fits to Eq. (3) we yield the fit-parameters listed in Tab. 1 (in any case we found $a = O(1)$ and a reduced chi-square $\chi^2_{\text{red}} \approx 1$). Hence, the transition points for all three setups agree within error bars and we subsequently denote the disorder value above which $\langle\omega_p\rangle < 0$ by $\rho_c^\omega = 0.285(1)$.

3.2. Configurational properties of MWPs at ρ_c^ω

We further performed simulations at the transition point $\rho_c^\omega = 0.285(1)$ to assess the scaling behavior of the root mean square (rms) fluctuations of the MWP weight $\delta\omega = [\langle\omega_p^2\rangle - \langle\omega_p\rangle^2]^{1/2}$, the average MWP length $\langle\ell\rangle$, and the average MWP roughness $\langle r\rangle$ (defined from the maximal extension of the MWP along the direction with the free BCs).

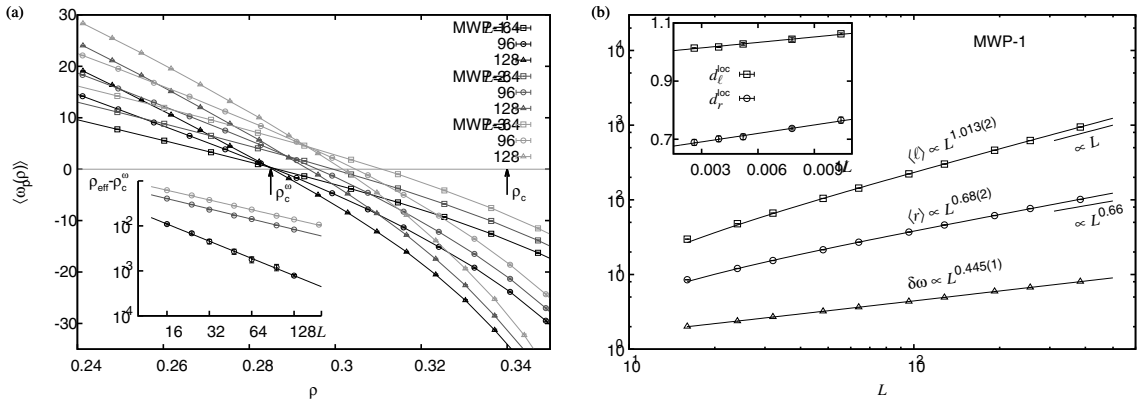

Fig. 4. Results of the finite-size scaling analysis for the MWP properties. (a) analysis of the ensemble averaged MWP weight $\langle\omega_p\rangle$. The main plot shows the raw data for the three MWP setups (see text for details; for a clear presentation only three system sizes are shown) and the inset illustrates the scaling behavior of the system size dependent characteristic values of $\rho_{\rm eff}(L)$, (b) finite-size scaling of the MWP observables at ρ_c^ω for the MWP-1 setup. The inset illustrates the extrapolation of the asymptotic scaling exponents from the local exponents for $\langle\ell\rangle$ and $\langle r\rangle$ (see text).

During the computation of the loops+MWP groundstate for a given realization of the disorder, the MWP weight, as part of the configurational weight of the MWPM on the auxiliary graph, is subject to optimization. As consequence, the distribution of MWP weights is skewed towards more negative weights and shows a good data collapse if rescaled according to $\mathrm{P}(\omega_\mathrm{p}) = \delta\omega^{-1}\mathrm{p}[\omega_\mathrm{p}/\delta\omega]$ (not shown). For the MWP observables we found best fits by considering scaling functions that account for deviations from the pure power-law scaling according to $\delta\omega \propto (L+\Delta L)^{d_\omega}$, $\langle\ell\rangle \propto (L+\Delta L)^{d_\ell}$, and $\langle r\rangle \propto (L+\Delta L)^{d_r}$, where we yield the scaling exponents listed in Tab. 1 (in either case we found $\Delta L = O(10)$ and $\chi^2_{\rm red} \approx 1$). As further numerical check we computed the effective (local) slopes that describe the scaling of an observable $\langle X\rangle$ within intervals of, say, m consecutive data points according to $\langle X\rangle \propto (L+\Delta L)^{d_X^{\rm loc}}$. By sliding this "scaling window" over the whole data set, one obtains a sequence of effective exponents $d_X^{\rm loc}(L)$. The asymptotic value d'_X is then extrapolated by means of a straight line fit to the plot of $d_X^{\rm loc}(L)$ as a function of the inverse system size. Here, for $m = 6$ we find $d'_\ell = 0.995(2)$ and $d'_r = 0.662(3)$.

These results suggest a self-affine scaling of the MWP at ρ_c^ω, in agreement with the geometric scaling exponents of the directed polymer in a random medium (DPRM) (Kardar and Zhang, 1987; Cieplak et al., 1994; Schwartz et al., 1998), characterized by $d_\ell = 1$ and $d_r = 2/3$. However, note that the rms fluctuation of the DPRM energy is governed by an exponent $d_\omega = 1/3$ (Kardar and Zhang, 1987) and we might hypothesize that the above value of $d_\omega = 0.445(1)$ is likely to be affected by the presence of the NWP critical point and that for smaller values of ρ one might find a crossover to the numeric value $1/3$. Indeed, further simulation at $\rho = 0.200$ yield the set of exponents $d_\omega = 0.34(1)$, $d_\ell = 1.008(1)$, and $d_r = 0.65(2)$ in excellent agreement with those that characterize the DPRM.

The discussion above focused on the analysis of the MWP-1 setup. We also performed similar analyses for the other two setups, summarized in Tab. 1. In either case we verified that in limit of weak disorder, i.e. at small values of ρ where the disorder averaged MWP weight $\langle\omega_\mathrm{p}\rangle$ is still larger than zero, the exponent d_ω assumes a value of ≈ 0.33 as for the DPRM.

Table 1. Transition points and scaling exponents that characterize the MWP observables at ρ_c^ω for the three considered MWP setups. From left to right: MWP setup, transition point ρ_c^ω, scaling exponent b (see Eq. 3), exponent d_ω that governs the scaling of the rms of the MWP weight fluctuations, length scaling exponent d_ℓ, roughness exponents d_r.

MWP setup	ρ_c^ω	b	d_ω	d_ℓ	d_r
MWP-1	0.285(1)	0.85(7)	0.445(1)	1.013(2)	0.68(2)
MWP-2	0.285(1)	1.32(8)	0.44(1)	1.006(6)	0.70(4)
MWP-3	0.287(1)	1.39(6)	0.445(1)	1.005(7)	0.659(5)

4. Summary

In Sects. 1 through 2.5 of the presented article we summarized existing literature on the NWP problem, i.e. a lattice-path model that features a disorder driven phase transition. A major part of the existing literature is focused on a "loops only" variant of the NWP model, wherein, for a given realization of the disorder, one is interested in the configurational properties of a minimum weight set of loops. A mapping of the NWP model to an associated combinatorial optimization problem allows to obtain such groundstate configurations by means of exact algorithms. Further, we also presented results for a "loops + minimum weight path (MWP)" variant of the NWP model, already introduced in Ref. (Melchert and Hartmann, 2008). In this case, the "loops + MWP" groundstates can be computed using a simple modification of the mapping procedure.

As function of a model intrinsic disorder parameter ρ the characteristic properties of the MWP change: for very small values of ρ, i.e. for a small fraction of negative edge weights on the underlying lattice, the disorder averaged configurational weight $\langle\omega_{\mathrm{p}}\rangle$ of the MWP is positive and the scaling behavior of the configurational weight and geometric MWP properties match those of the directed polymer in a random medium (DPRM) (Kardar and Zhang, 1987), exhibiting the scaling behavior of a self-affine lattice path. As ρ exceeds a first threshold value $\rho_{\mathrm{c}}^{\omega} = 0.285(1)$ (the numerical value is characteristic for the Gaussian-like disorder distribution studied here, for a bimodal disorder distribution one finds $\rho_{\mathrm{c}}^{\omega} = 0.0869(2)$, see Ref. (Melchert and Hartmann, 2008)), $\langle\omega_{\mathrm{p}}\rangle$ turns negative and the geometric properties are still in agreement with those of the DPRM. At the NWP critical point $\rho_{\mathrm{c}} = 0.340(1)$ (for a bimodal disorder distribution one has $\rho_{\mathrm{c}} = 0.1028(3)$), the geometric properties of the loops and paths change, indicating a self-similar scaling behavior with scaling exponents that agree well with those found in the context of the optimal path problem (Schwartz et al., 1998). Also note that in $3d$ all the critical exponents of the NWP problem appear to be quite close to those that describe the strongly screened vortex glass model (Pfeiffer and Rieger, 2002). As soon as the disorder parameter ρ exceeds the NWP critical point ρ_{c} and approaches the limit $\rho = 1$, the geometric properties of the "loops only" variant of the NWP model agree well with those of fully packed loops in the "random manifold" and "random elastic medium" discrete interface models (Zeng et al., 1998).

In summary, the NWP problem constitutes an interesting non-standard optimization percolation problem with a rich critical behavior and various limiting cases that, on their own, represent intriguing problems studied in the context of the statistical physics of disordered systems.

Acknowledgements

OM gratefully acknowledges financial support from the DFG (*Deutsche Forschungsgemeinschaft*) under grant HA3169/3-1. The simulations were performed at the HPC Cluster HERO, located at the University of Oldenburg (Germany) and funded by the DFG through its Major Instrumentation Programme (INST 184/108-1 FUGG) and the Ministry of Science and Culture (MWK) of the Lower Saxony State.

References

Ahuja, R.K., Magnanti, T.L., Orlin, J.B., 1993. Network Flows: Theory, Algorithms, and Applications. Prentice Hall.

Allega, A.M., Fernández, L.A., Tarancón, A., 1990. Configurational statistics of strings, fractals and polymer physics. Nucl. Phys. B 332, 760.

Antunes, N.D., Bettencourt, L.M.A., 1998. The Length Distribution of Vortex Strings in $U(1)$ Equilibrium Scalar Field Theory. Phys. Rev. Lett. 81.

Apolo, L., Melchert, O., Hartmann, A.K., 2009. Phase transitions in diluted negative-weight percolation models. Phys. Rev. E 79, 031103.

Austin, D., Copeland, E.J., Rivers, R.J., 1994. Statistical mechanics of strings on periodic lattices. Phys. Rev. D 49, 4089.

Camarda, M., Siringo, F., Pucci, R., Sudbø, A., Hove, J., 2006. Methods to determine the Hausdorff dimension of vortex loops in the three-dimensional XY model. Phys. Rev. B 74, 104507.

Cardy, J., 2005. SLE for Theoretical Physicists. Ann. of Phys. 318, 81.

Cieplak, M., Maritan, A., Banavar, J.R., 1994. Optimal paths and domain walls in the strong disorder limit. Phys. Rev. Lett. 72, 2320.

Claussen, G., Apolo, L., Melchert, O., Hartmann, A.K., 2012. Analysis of the loop length distribution for the negative-weight percolation problem in dimensions $d = 2$ through $d = 6$. Phys. Rev. E 86, 056708.

Cook, W., Rohe, A., 1999a. For the calculation of minimum-weighted perfect matchings we use Cook and Rohe's blossom4 extension to the Concorde library, http://www2.isye.gatech.edu/ wcook/blossom4/.

Cook, W., Rohe, A., 1999b. Computing minimum-weight perfect matchings. INFORMS J. Computing 11, 138–148.

Derrida, B., 1990. Directed polymers in a random medium. Physica A 163, 71.
Grassberger, P., 1993. Recursive sampling of random walks: self-avoiding walks in disordered media. J. Phys. A 26, 1023.
Hartmann, A.K., 2007. Domain walls, droplets and barriers in two-dimensional ising spin glasses, in: W, J. (Ed.), Rugged Free Energy Landscapes, Springer, Berlin. pp. 67 – 106.
Hartmann, A.K., Rieger, H., 2001. Optimization Algorithms in Physics. Wiley-VCH, Weinheim.
Hindmarsch, H., Strobl, K., 1995. Statistical properties of strings. Nucl. Phys. **B** 437, 471.
Kajantie, K., Laine, M., Neuhaus, T., Rajantie, A., Rummukainen, K., 2000. O(2) symmetry breaking versus vortex loop percolation. Phys. Lett. B 482, 114 – 122.
Kardar, M., Zhang, Y.C., 1987. Scaling of Directed Polymers in Random Media. Phys. Rev. Lett. 58, 2087.
Kremer, K., 1981. Self-Avoiding-Walks (SAW's) on Diluted Lattices, a Monte Carlo Analysis. Z. Phys. B 45, 149.
Melchert, O., 2009. PhD thesis. not published.
Melchert, O., Apolo, L., Hartmann, A.K., 2010. Upper critical dimension of the negative-weight percolation problem. Phys. Rev. E 81, 051108.
Melchert, O., Hartmann, A.K., 2007. Fractal dimension of domain walls in two-dimensional Ising spin glasses. Phys. Rev. B 76, 174411.
Melchert, O., Hartmann, A.K., 2008. Negative-weight percolation. New. J. Phys. 10, 043039.
Melchert, O., Hartmann, A.K., 2011a. A dedicated algorithm for calculating ground states for the triangular random bond Ising model. Comp. Phys. Comm. 182, 1828.
Melchert, O., Hartmann, A.K., 2011b. Configurational statistics of densely and fully packed loops in the negative-weight percolation model. Eur. Phys. J. B 80, 155–165.
Melchert, O., Hartmann, A.K., 2013. Typical and large-deviation properties of minimum-energy paths on disordered hierarchical lattices. Eur. Phys. J. B 86, 323.
Melchert, O., Hartmann, A.K., Mézard, M., 2011. Mean-field behavior of the negative-weight percolation model on random regular graphs. Phys. Rev. E 84, 041106.
Mitran, T.L., Melchert, O., Hartmann, A.K., 2013. Biased and greedy random walks on two-dimensional lattices with quenched randomness: The greedy ant within a disordered environment. Phys. Rev. E 88, 062101.
Nguyen, A.K., Sudbø, A., 1998. Onsager loop transition and first-order flux-line lattice melting in high-T_c superconductors. Phys. Rev. B 57, 3123–3143.
Nguyen, A.K., Sudbø, A., 1999. Topological phase fluctuations, amplitude fluctuations, and criticality in extreme type-ii superconductors. Phys. Rev. B 60, 15307–15331.
Norrenbrock, C., Melchert, O., Hartmann, A.K., 2013. Paths in the minimally weighted path model are incompatible with Schramm-Loewner evolution. Phys. Rev. E 87, 032142.
Papadimitriou, C., Steiglitz, K., 1998. Combinatorial Optimization – Algorithms and Complexity. Dover Publications Inc., Mineola, NY.
Parshani, R., Braunstein, L.A., Havlin, S., 2009. Structural crossover of polymers in disordered media. Phys. Rev. E 79, 050102.
Pfeiffer, F.O., Rieger, H., 2002. Superconductor-to-normal phase transition in a vortex glass model: numerical evidence for a new percolation universality class. J. Phys.: Condens. Matter 14, 2361.
Pfeiffer, F.O., Rieger, H., 2003. Critical properties of loop percolation models with optimization constraints. Phys. Rev. **E** 67, 056113.
Rieger, H., 2003. Polynomial combinatorial optimization methods for analysing the ground states of disordered systems. J. Phys. A 36.
Schakel, A.M.J., 2001. Percolation, Bose-Einstein condensation, and string proliferation. Phys. Rev. E 63, 026115.
Schwartz, N., Nazaryev, A.L., Havlin, S., 1998. Optimal path in two and three dimensions. Phys. Rev. E 58, 7642.
Schwarz, K., Karrenbauer, A., Schehr, G., Rieger, H., 2009. Domain walls and chaos in the disordered SOS model. J. Stat. Mech. 2009, P08022.
Stauffer, D., 1979. Scaling theory of percolation clusters. Phys. Rep. 54, 1–45.
Stauffer, D., Aharony, A., 1994. Introduction to Percolation Theory. Taylor and Francis, London.
Strobl, K., Hindmarsh, M., 1997. Universality and critical phenomena in string defect statistics. Phys. Rev. E 55, 1120–1149.
Zeng, C., Kondev, J., McNamara, D., Middleton, A.A., 1998. Statistical Topography of Glassy Interfaces. Phys. Rev. Lett. 80, 109–112.